On the Structure of Transition-Metal Nitrogen Complexes‡

Eval Rud Møller and Karl Anker Jørgensen*

Department of Chemistry, Aarhus University, DK-8000 Århus C, Denmark

Møller, E. R. and Jørgensen, K. A., 1991. On the Structure of Transition-Metal Nitrogen Complexes. – Acta Chem. Scand. 45: 68–76.

The structures of linear, bent and side-on coordinated dinitrogen fragments to transition metals have been investigated using the frontier orbital approach. The linear M–N–N structures are discussed on the basis of $ReCl_2(PR_3)_3NNR'$; the main interactions between the NNR'^- fragment and the $ReCl_2(PR_3)_3^+$ fragment are between the antibonding π^*_{N-N} orbitals and the metal d_{xz} and d_{yz} orbitals. The bent structures are discussed on the basis of $RhCl(PR_3)_3NNR'^+$. The essential difference between the linear and the bent M–N–N complexes is the presence of a two-orbital four-electron interaction in the latter type of complexes, which causes the long M–N bond lengths for the bent complexes compared with the linear ones. Other types of linear and bent complexes are discussed, and also complexes with both a linear and a bent M–N–N functionality are analyzed. The orbital population and atomic charge changes when moving from a linear to a bent M–N–N structure are also discussed. The reactivity of some M–N–N complexes is also presented. The side-on coordinated $M(NR-NR_2)$ structures are analyzed for complexes containing either a d^0 or a d^2 metal.

There has been increased interest among chemists over the last two decades in finding methods for the activation of strong bonds in small molecules, such as molecular nitrogen and molecular oxygen. The interest in the activation of molecular oxygen has been manifold: including the mechanism of the activation and the potential to carry out oxidation reactions with molecular oxygen as the oxygen source.[1–3] With regard to the activation of molecular nitrogen the understanding of its reduction to ammonia, which is catalyzed by nitrogenase enzymes has been of prime importance.[4,5]

In an attempt to gain insight into the activation of molecular nitrogen a lot of attention has been devoted to transition-metal complexes that react with molecular nitrogen or various nitrogen compounds. Consequently a variety of transition-metal complexes with different nitrogen functionalities have been prepared and characterized by X-ray crystallography.[4,5] One group of transition-metal nitrogen complexes contains the diazenido unit, M–N–N–R, which serves as a model to mimic the first intermediate on the route to the reduction of molecular nitrogen to ammonia. The transition-metal diazenido unit may display a number of conformations depending on the substituents on the nitrogens, on the transition metal and on the co-ligands. It can adopt a 'linear' conformation, **Ia**,[6–14] or a 'bent' conformation, **Ib**.[15,16]

Protonation or alkylation of the β-nitrogen of the diazenido ligand leads to the 'linear,' **IIa**,[6,7,17–21] or the 'bent,' **IIb**,[9,10,22,23] hydrazido (2–) or 'isodiazene' ligand. If the α-nitrogen is protonated, the result is the 'diazene' (**IIc**) ligand.[16,24] Doubly protonated diazenido ligands may obtain a 'diazene'-like structure, **IIIa**,[11,25,26] with double bond character between the two nitrogens, or a hydrazido (1–) ligand structure with a single N–N bond. The latter can coordinate either in an 'end on' (**IIIb**)[6,12,17] or a 'side on' manner (**IIIc**).[12,13,18,27–30]

An example of each of the eight basis structures, depicted in Fig. 1, is shown in **1–8**, with the M–N and N–N bond lengths and MNN bond angles given as well.[6,7,12,15,16,22,25]

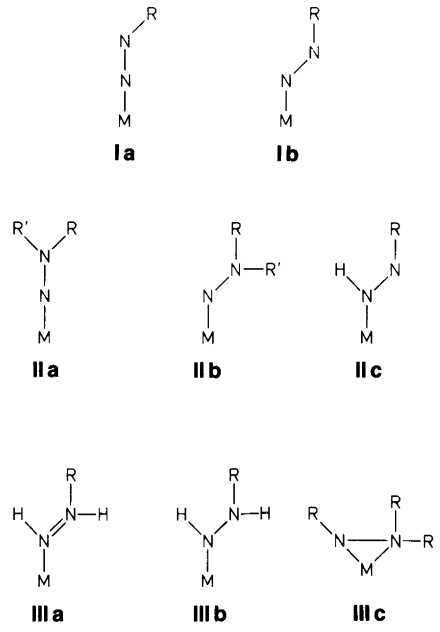

Fig. 1. Different structural conformations of transition-metal nitrogen complexes.

* To whom correspondence should be addressed.

‡ Dedicated to Egill Jacobsen on the occasion of his 80th birthday.

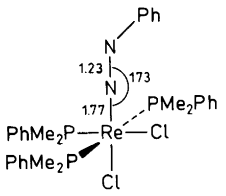

1

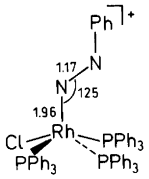

2

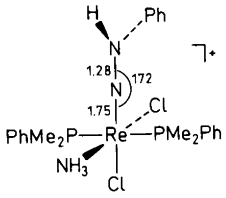

3

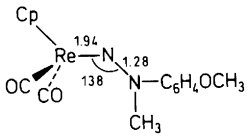

4

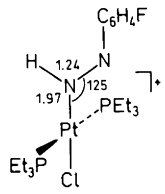

5

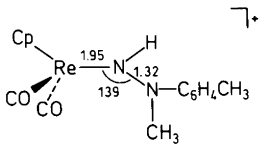

7

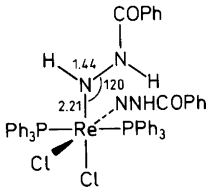

7

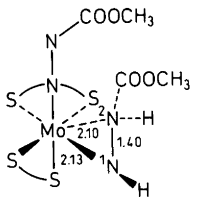

8

Inspection of the N–N bond lengths for the different types of complex **1–8** shows that they vary from being triple–double-bond-like in **2** (1.17 Å) to single-bond-like in **7** (1.44 Å). The M–N bond length varies from 1.75 Å in **3** to 2.21 Å in **7**. Several interesting trends appear from the structures of the transition-metal nitrogen complexes: (i) the linear M–N–N complexes have shorter M–N bond lengths than the corresponding bond in the bent M–N–N complexes, (ii) different nitrogen protonation/alkylation sites are observed and (iii) for complexes with two similar ligands, the M–N–N bending angle influences both the M–N and N–N bond lengths.

A series of complexes in which both a linear and a bent M–N–N fragment are present have also been characterized.[6,10,11] Two examples are shown, **7** and **9**. The Re–^{1}N

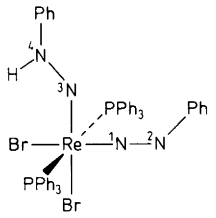

9

and Re–^{3}N bond lengths are 1.79 and 1.92 Å in **9**, and the ^{1}N–^{2}N and ^{3}N–^{4}N bond lengths are 1.21 and 1.29 Å, respectively. The angle Re^{1}N^{2}N is 172° and the angle Re^{3}N^{4}N is 131°.

One might wonder why these differences in the structure of the M–N–N fragments exist and why different nitrogen protonation/alkylation sites are observed. Some of the differences can be attributed to the number of electrons on the metal whereas others are not so obvious. In the present work we attempt to gain a better understanding of the different types of structure of the different transition-metal nitrogen complexes shown in Fig. 1 and, to a certain extent, try to explain some of their reactions. To this end, we have used theoretical calculations based on extended Hückel theory and on fragment molecular orbital (FMO) analysis.[31] It is our intention to analyze the interaction between the metal and nitrogen fragments for the different types of complex within the FMO framework. Our work is not the first in which transition-metal dinitrogen complexes are considered theoretically,[32–34] but to our knowledge it is the first time that the types of complex in Fig. 1 exemplified by **1–9** are considered in a theoretical analysis.

Results

Linear M–N–N structures. Let us start with the electronic structure of the linear M–N–N fragments of the type **Ia**. The interaction between the N–N–R and the transition-metal fragment is analyzed by means of an interaction diagram. The different linear structures can be understood by viewing the results of our calculation on the ReCl^2(PR$_3$)$_3$NNR′, **1**. For the 18-electron rule to be fulfilled, the diazenido fragment in **1** must be considered as a three-electron donor. The interaction diagram is shown in Fig. 2, with the $ReCl_2(PR_3)_3^+$ fragment shown to the left and the NNR′$^-$ fragment to the right.

The $ReCl_2(PR_3)_3^+$ fragment has two nearly degenerate levels at −12.25 eV. These are the d_{yz} and d_{xy} orbitals, and both are occupied, making up the highest occupied molecular orbitals (HOMOs) for the system. Right above these, at −12.07 eV, is located the lowest unoccupied molecular orbital (LUMO), d_{xz}. At −10.64 eV is found a hybrid orbital of d_{z^2}, p_z and s, and higher in energy at −5.56 eV is

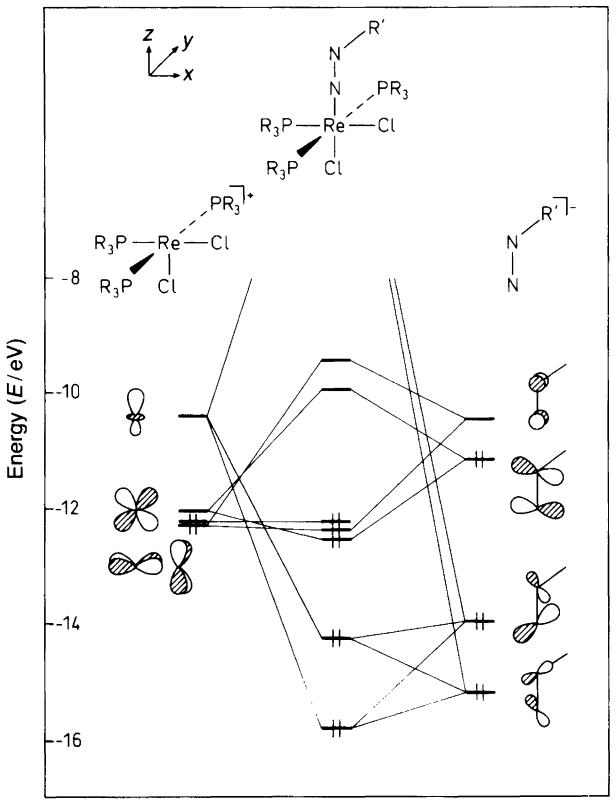

Fig. 2. Interaction diagram for the $ReCl_2(PR_3)_3NNR'$ from $ReCl_2(PR_3)_3^+$ and NNR'^-.

the $d_{x^2-y^2}$ orbital (not shown in Fig. 2). The HOMO of the NNR'^- fragment at −11.16 eV is of p_x symmetry, and is antibonding between the two nitrogens. Two orbitals made from a mixing of $p_x \pm p_z$, bonding between the two nitrogens, are located at −13.95 and −15.17 eV, with the antibonding combinations found above the LUMO shown in Fig. 2. The LUMO is the π^*_{N-N} of p_y symmetry at −10.46 eV. The primary interactions in $ReCl_2(PR_3)_3NNR'$ (**1**) are the HOMO–LUMO interactions. The π_y^* LUMO of the NNR'^- fragment interacts with the Re HOMO d_{yz} orbital, and the π_x^* HOMO of the NNR'^- fragment interacts with the Re LUMO d_{xz} orbital. The two occupied π_{N-N} orbitals of the NNR'^- fragment, lower in energy, interact with the metal d_{z^2} hybrid orbital. The LUMO of the NNR'^- fragment accepts 0.51 electrons from the d_{yz} orbital of the metal fragment, whereas the HOMO of the NNR'^- fragment donates 1.22 electrons to the metal by the interaction with the d_{xz} orbital. The interactions outlined in Fig. 2 lead to a transfer of 1.31 electrons from the nitrogen fragment to the metal fragment.

The HOMO of **1** is mainly Re d_{xy} and is not of interest, since it does not participate in the interaction with the NNR'^- fragment. Directly below the HOMO are located the second and third HOMOs. The third HOMO in **3** evidently forms the π-bond between the two fragments, as can easily be seen from Fig. 3.

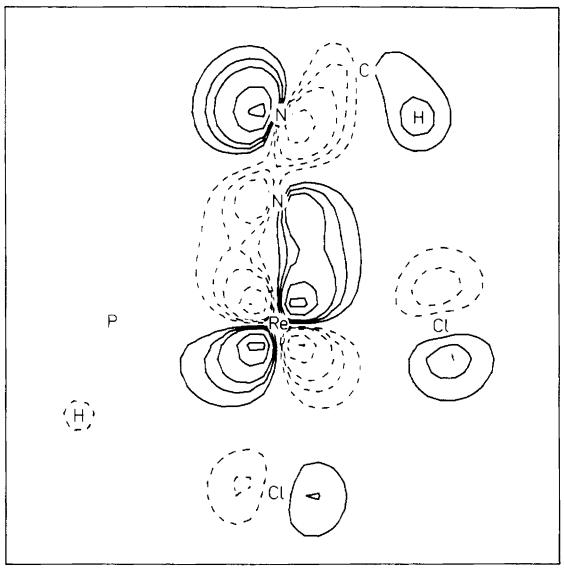

Fig. 3. Plot of the third HOMO of $ReCl_2(PR_3)_3NNR'$. The contours ψ are: 0.04, 0.07, 0.10, 0.20 and 0.30. The orbital is plotted in the *xz* plane.

The second HOMO, also a π-type of orbital, is perpendicular to the Re−N π-bond depicted in Fig. 3. It is mainly composed of the interaction of the d_{yz} orbital between the metal center and π_y^* orbital of the diazenido unit. There is also a minor contribution from the π_y orbital, which diminishes the amplitude on the α-nitrogen and enhances the amplitude on the β-nitrogen. Thus the second HOMO can be regarded as a pseudo-allylic system, as depicted in **10**.

The third HOMO depicted in Fig. 3 also has a higher amplitude on the β-nitrogen (0.560) than on the α-nitrogen (0.281). The atomic charges of the two nitrogens in **1** are also different, with a charge of 0.36 on the α-nitrogen and −0.34 on the β-nitrogen. Therefore, from both an orbital and a charge point of view, it seems reasonable that the β-nitrogen is more nucleophilic than the α-nitrogen, and that this type of complex will react with electrophiles at the β-nitrogen. This has been found for **3**, a type **IIa** complex, which is protonated at the β-nitrogen. The protonation of the β-nitrogen leading to **3** should be expected not to affect the N−N and M−N bond lengths significantly compared with **1**, as very little amplitude is found at the α-nitrogen.

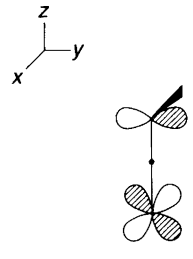

10

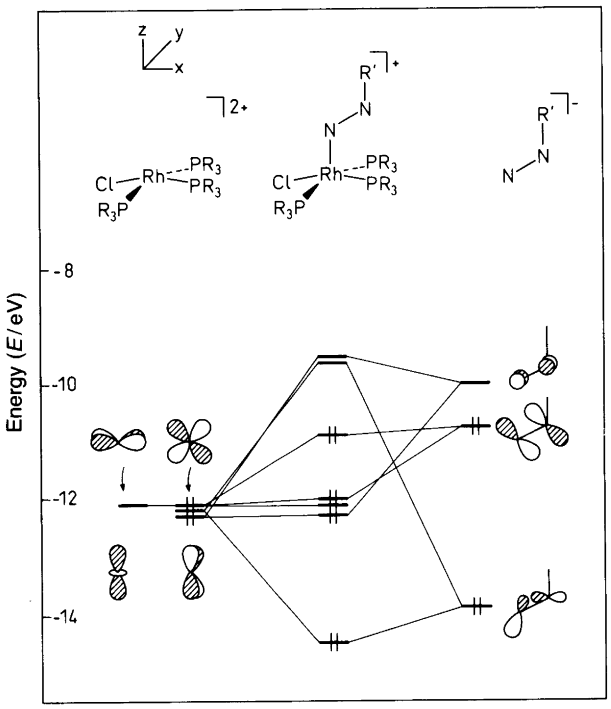

Fig. 4. Interaction diagram for the $RhCl(PR_3)_3NNR'^+$ from $RhCl(PR_3)_3^{2+}$ and NNR'^-.

This is also in accordance with the observed structures for the type **Ia** and **IIa** complexes.[6-14,17-21] We have also found that the bonding picture given here for the linear M–N–N–R′ structure is also valid for the trigonal bipyramidal rhenium and technetium complexes (not shown here).[8,9] Therefore all the complexes containing a linear M–N–N framework may be grouped together.

Bent M–N–N structures. Let us continue with the **Ib** complexes in which the M–N–N angle is bent. We have, as a starting point, chosen **2** as a model for these types of complex. The phenyldiazenido fragment in this complex can be considered as a two-electron donor. The interaction diagram for $RhCl(PR_3)_3NNR'^+$ is shown in Fig. 4, with the $RhCl(PR_3)_3^{2+}$ fragment shown to the left and the NNR'^- fragment to the right.

The $RhCl(PR_3)_3^{2+}$ fragment has four MOs located very close in energy of d_{yz}, d_{z^2}, d_{xz} and d_{xy} symmetry at about −12.25 eV. These four orbitals are occupied by six electrons. Several eV higher in energy is placed the $d_{x^2-y^2}$ orbital at −4.60 eV (not shown in Fig. 4). The frontier orbitals of the NNR'^- fragment to the right are similar to those shown in Fig. 2. The occupied Rh d_{yz} orbital interacts with the LUMO π^*_{N-N} of p_y symmetry of the nitrogen fragment. The HOMO of the NNR'^- fragment, a combination of p_x and p_z, which is antibonding between the nitrogens, interacts with the d_{xz} orbital at the metal, to give the bonding and antibonding Rh–N combinations, both occupied by two electrons, shown in the middle of Fig. 4. The Rh d_{z^2} orbital interacts with the N–N bonding orbital located at −13.89 eV. Through the interaction of the NNR'^- fragment with the $RhCl(PR_3)_3^{2+}$ fragment, the LUMO of the former fragment accepts 0.25 electrons from the metal, whereas the HOMO and the second HOMO donate 0.59 and 0.25 electrons, respectively, to the metal. The NNR'^- fragment donates in total 0.74 electrons to the metal by the interaction leading to **2**, which is 0.57 electrons less than the interaction between the NNR'^- fragment and the metal leading to **1**. The frontier orbitals for the various Re complexes with a bent Re–N–N fragment also lead to an orbital picture with the antibonding Re–N orbital occupied by two electrons as the HOMO.

It appears from the interaction diagram, shown in Fig. 4, that the HOMO of **2** is the antibonding Rh–N orbital. This orbital is shown in Fig. 5, where the antibonding character is visualized.

Comparison of the frontier orbitals of **1** and **3** with **2** reveals an explanation for the difference in M–N bond lengths; in the former type of complex an antibonding M–N orbital is the LUMO of the system, whereas for the bent type of complex the antibonding M–N orbital is occupied, which causes the longer M–N bond length in the latter case. The reason for the short N–N bond in **2** compared with **1** and **3** is a mixing of nitrogen s-character into the π^*_{N-N} orbitals, as depicted in **11**, by which the antibonding character is diminished.

Another difference between the two types of fragment is the electron donation; the linear N–N–R′ fragment donates 1.31 electrons to the metal fragment, whereas the bent fragment donates only 0.74 electrons. The remaining electron density in the latter case is located on the α-nitrogen which has a charge of −0.24 (compared with 0.36 in **1**), whereas the β-nitrogen has nearly the same charge in **2** (−0.31) as in **1** (−0.34).

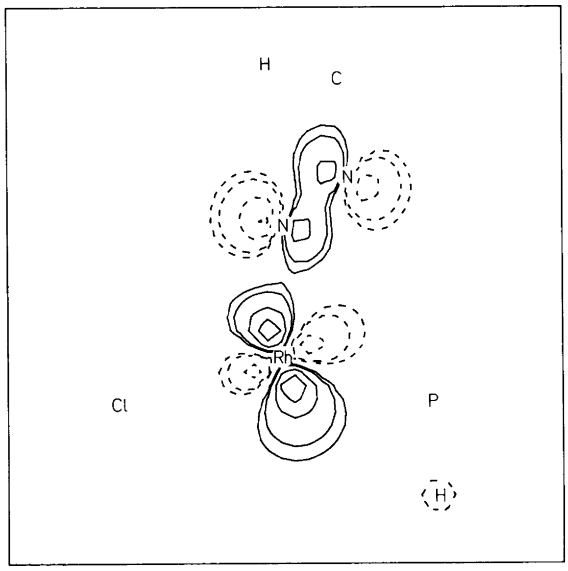

Fig. 5. Plot of the HOMO of $RhCl(PR_3)_3NNR'^+$. The contours ψ are: 0.07, 0.10, 0.20 and 0.30. The orbital is plotted in the *xz* plane.

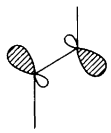

11

The frontier orbitals and the charge consideration of **2** indicate that the reactions of the bent type of M–N–N complex with electrophiles can lead to reaction at both the α-nitrogen and the β-nitrogen as they have nearly the same net charge and amplitude in the HOMO (0.638 on the α-nitrogen and 0.583 on the β-nitrogen). It should thus be expected that changes in the R′-substituent in the N–N–R′ part of the complex might cause a change in reaction at the α-nitrogen or the β-nitrogen of the bent M–N–N–R′ complexes with electrophiles. This phenomenon is observed in **4** and **5**. In **4**, in which a 4-methoxyphenyl group is attached to the β-nitrogen, the β-nitrogen is protonated because of the electron-donating properties of the substituent which increases the electron density at the β-nitrogen, whereas in **5**, where the substituent contains an electron-withdrawing group – the 4-fluorophenyl group, the protonation site is the α-nitrogen.

Let us finish this section with a discussion of the difference between **6** and **7**, which are complexes substituted on both the α- and the β-nitrogen. The major difference in the bonding picture of these two complexes is the Re–N and N–N bond lengths. The rhenium atom in **6** is in an irregular tetrahedral environment, which causes a mixing of the d-orbitals into the three over two situation, whereas in **7**, it is coordinated in an octahedral manner, with the metal orbitals two over three.

Because of the different electronic environments at the metal center in **6** and **7**, the interaction patterns between the metal orbitals and the nitrogen fragment orbitals change. The interaction diagrams are shown in Fig. 6, where only the major interactions are depicted. To the left is the interaction diagram for **6**, and to the right is that for **7**.

For the $CpRe(CO)_2^{2+}$ fragment to the left are shown d_{yz} orbital and the two orbitals resulting from a mixing of the d_{xz} and d_{z^2} orbitals. The d_{yz} orbital is the LUMO, and the two others make the HOMO and a second LUMO. In the $ReCl_2(PR_3)_2NNHCH_3^+$ fragment to the right, the ordering of the orbitals is reversed, such that the HOMO is d_{yz} and the two mixed orbitals are unoccupied. The two orbitals outlined for the $NHNRR'^-$ fragment, in the middle, are the antibonding π^*_{N-N} of *y* and *z* character.

The interaction between the two orbitals arising of d_{xz} and d_{z^2} and the π_z^* orbital on the nitrogen fragment forms the three expected orbitals, namely a Re–N bonding, a non-bonding and an antibonding orbital. The Re–N and N–N overlap populations are not significantly affected whether the non-bonding orbital is filled (**6**) or not (**7**). Thus the d_{yz}–π^*_{y-N-N} orbital interaction is solely responsible for the bond-length differences observed for **6** and **7**.

For **6** we observe a two-orbital two-electron interaction between the d_{yz} on the metal fragment and the π^*_{y-N-N} on the nitrogen fragment. Through this interaction, the π^*_{y-N-N} orbital donates 1.4 electrons to the metal. This leads to a shorter N–N bond because of the depletion of electrons from an antibonding π^*_{y-N-N}. Furthermore, this orbital interaction has a π-bonding feature between the Re and N, which accounts for the shorter Re–N bond length found in **6**.

For **7** the same orbitals make a two-orbital four-electron interaction. This interaction prevents electron donation from the π^*_{y-N-N} orbital to the metal. The π^*_{y-N-N} orbital is thus filled in **7**, which causes the longer Re–N and N–N bond lengths observed.

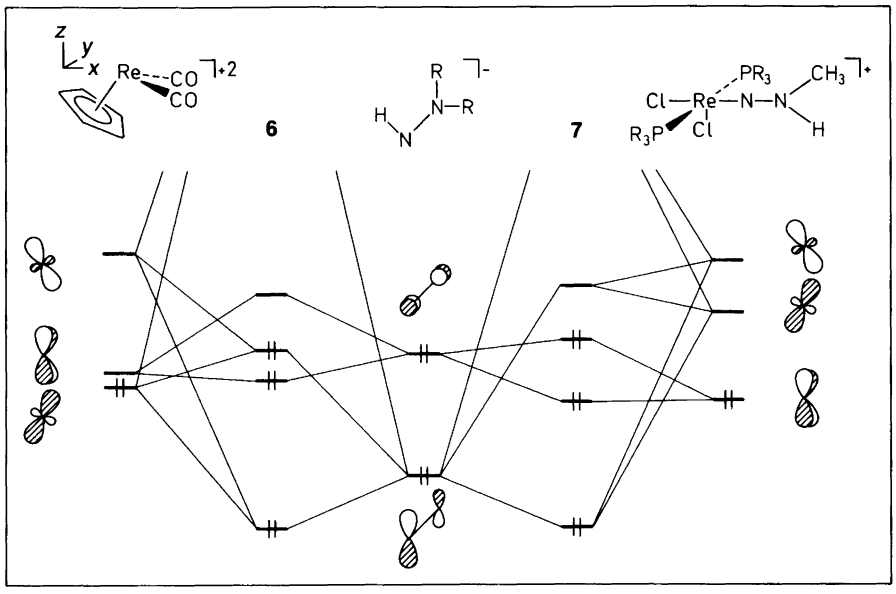

Fig. 6. A partial interaction diagram for **6** to the left and for **7** to the right.

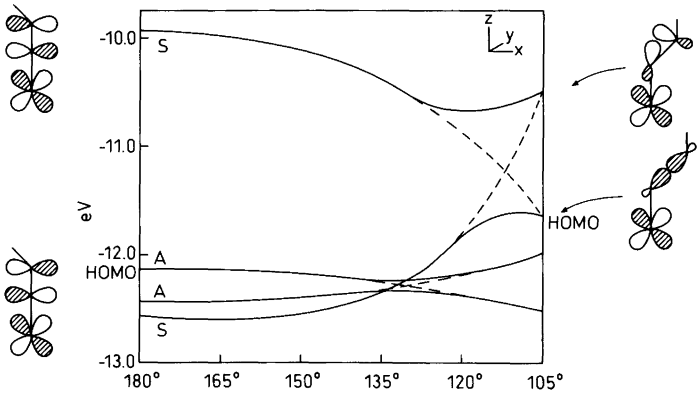

Fig. 7. Correlation diagram for bending at the β-nitrogen in $ReCl_2(PR_3)_3NNR'$.

Linear-bent M–N–N structures. A series of complexes in which both a linear and bent M–N–N fragment is present has also been found and characterized; two examples are **7** and **9**. We have performed calculations for different types of these complexes. The interactions outlined above for the 'isolated' linear and the bent M–N–N fragment with a metal fragment are also found for such complexes. We suggest that the reason for the presence of a linear and a bent M–N–N fragment in these types of complex is to fulfil the 18-electron rule.

From linear to bent M–N–N structures. The interaction diagrams for the linear and bent forms of the diazenido complexes show a different ordering of the frontier orbitals. We will, in the following, account for this difference in terms of an orbital correlation diagram. The correlation diagram for the bending of the M–N–N fragment in **1** from 180° to 105° is shown in Fig. 7 where the orbitals are classified as symmetric/antisymmetric with respect to the mirror plane.

Two avoided crossings are observed in Fig. 7; one is between the HOMO and the second HOMO, both antisymmetric, at about 130°. The other, between two symmetric orbitals, occurs at about 115°. The two antibonding orbitals which are orthogonal to the plane of the bending are only slightly affected. The largest change in energy is found for the orbitals in the plane of the bending. The orbital which is bonding between the metal and the α-nitrogen and antibonding between the two nitrogens is destabilized by the bending, while the orbital which is antibonding between all three atoms is stabilized.

The changes in orbital energy between the two symmetric orbitals can be traced to changes in overlap population between the atoms of the M–N–N fragment. The LUMO, which crosses the HOMO of the system, is a hybrid of some s and p_z character as a results of the bending, and, in the product, this initially π-antibonding N–N orbital changes to a σ_{N-N} orbital, shown to the right in the correlation diagram. The LUMO of the bent structure also shows some N–N bonding character, but not as much as the HOMO. The LUMO is also shown to the right in Fig. 7. It should be pointed out that the avoided crossings in Fig. 7 occur at a rather late stage of the bending, due to the fact that no changes in bond length of the linear M–N–N–R′ fragment take place upon bending. Furthermore, by adjusting the bond lengths of the bent framework of **1**, according to the known structures, an interchange of some of the occupied orbitals takes place, to give an orbital picture matching that observed for the bent M–N–N–R′ structure, **2**.

We also calculated the change in overlap population between Re–N and N–N as a function of the bending angle and the results are shown in Fig. 8.

Two interesting observations can be made from Fig. 8. At the point where the avoided crossing takes place, the N–N overlap population increases from 1.190 at 135° to 1.283 at 105°, whereas the Re–N overlap population decreases from 0.817 to 0.487 for the same change in angle. These changes account then for the increase in Re–N and decrease in N–N bond lengths, on going from a linear to a bent M–N–N–R′ complex.

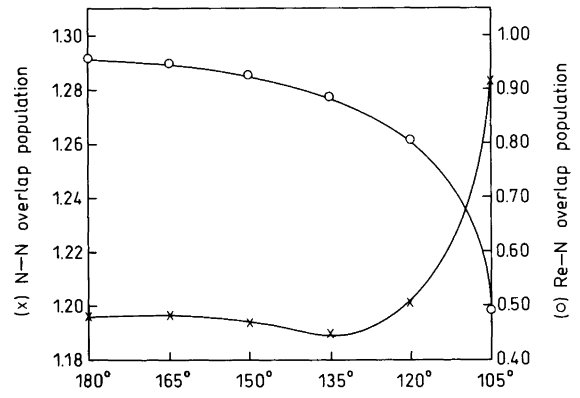

Fig. 8. Change in N–N and Re–N overlap populations as a function of the bending at the β-nitrogen in $ReCl_2(PR_3)_3NNR'$.

Side-on coordinated M(NR–NR$_2$) structures. The interaction diagram for the type **IIIc** complexes, represented by **8**, is shown in Fig. 9. The $Mo(N_2R)(SR)_2^+$ fragment is shown to the left and the $HNNHR'^-$ fragment to the right.

Complex **8** can, to a certain extent, be compared to a

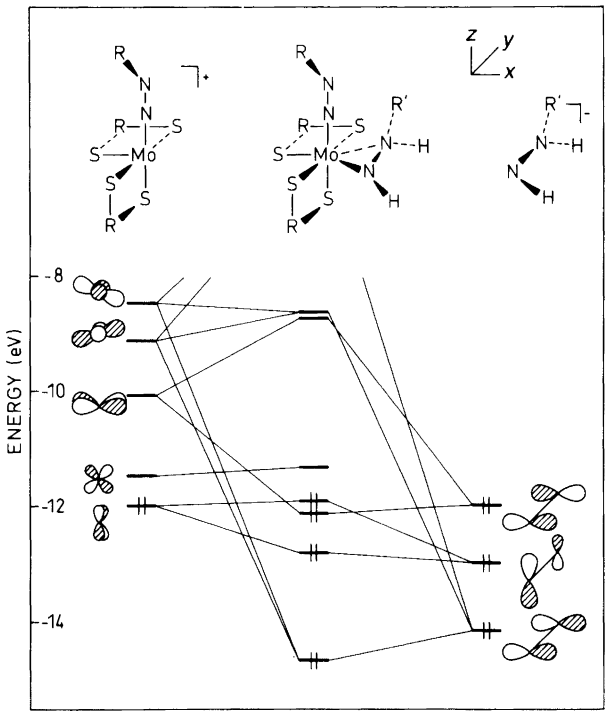

Fig. 9. Interaction diagram for the formation of $Mo(dmtc)_2(NNCO_2Me)(\eta^2\text{-}NHNHCO_2Me)$ from $Mo(dmtc)_2(NNCO_2Me)^+$ and $\eta^2\text{-}NHNHCO_2Me^-$.

bidentate coordinated peroxide which has been characterized by X-ray crystallography.[35] The interaction diagram for **8** shows some similarities to that presented for bidentate coordinated peroxide.[36] The HOMO of the $Mo(N_2R)(SR)_2^+$ fragment, the d_{yz} orbital, interacts with the second HOMO of the $HNNHR'^-$ fragment, the π^*_{N-N} orbital of p_z symmetry, in a two-orbital four-electron δ-type interaction. This results in the occupation of the bonding as well as the and antibonding combinations. The second LUMO of the metal fragment, the d_{xy} orbital, interacts with the π^*_{N-N} orbital of p_x symmetry (the HOMO); and, furthermore, an unoccupied molecular orbital located higher in energy at the $Mo(N_2R)(SR)_2^+$ fragment interacts with the π_{N-N} orbital of p_x symmetry of the $HNNNR'^-$ fragment. The interaction of the two fragments in Fig. 9 leads to donation of 0.86 electrons from $HNNHR'^-$ to the $Mo(N_2R)(SR)_2^+$ fragment. The main interaction is the Mo-d_{xy}–π^*_{N-N} by which 0.55 electrons are donated to the metal. It is interesting to note the difference in the interactions between a bidentate coordinated peroxide/peroxo fragment and a bidentate coordinated hydrazido fragment. In the interaction between the peroxo fragment and an Mo-complex two lone-pair combinations are formed at the per-oxygens; one is oriented parallel and one perpendicular to the metal–peroxo plane.[36a] The frontier orbitals and the interaction diagram in Fig. 9 indicate that such lone pairs are not formed in the same significant way in **8** compared with the bidentate coordinated peroxo-d^0-metal complexes. Changing to a d^0-metal complex with a side-on coordinated hydrazido ligand, as, e.g., in $CpCl_2Ti[CH_3NN(CH_3)_2]$, the interaction diagram changes slightly for the interaction between $CpCl_2Ti^+$ and $CH_3NN(CH_3)_2^-$ compared with that shown in Fig. 9. The interaction diagram of the $CpCl_2Ti[CH_3NN(CH_3)_2]$ complex leads to an orbital picture, in which the π_{N-N} orbitals of p_x and p_y symmetry do not interact significantly with the Ti d-orbitals and thus are nearly lone-pair combinations on the nitrogen ligands in the complex. The metal of **8** and of $CpCl_2Ti[CH_3NN(CH_3)_2]$ are in two different oxidation states. In the former a d^2 molybdenum complex is found, whereas Ti is d^0 in the latter case. The change in the metal is evident from the net charges at the nitrogens in the $R'NNR'_2$ fragment, the charge on the singly substituted nitrogen in **8** is −0.86, whereas it is −0.40 in $CpCl_2Ti[CH_3NN(CH_3)_2]$ and for the doubly substituted nitrogen the charges are 0.00 and −0.19, respectively.

Discussion

Let us in the following discuss the results obtained in relation to the different types of interaction and to the bindings of the N–N–R fragment to the metal, as depicted in Scheme 1. From Fig. 1, eight types of complex are considered. Using a frontier orbital approach, it is probably more appropriate and convenient to consider only three types of N–N–R structure: (i) linear, (ii) bent and (iii) side-on.

The interaction diagram for the frontier orbitals of the linear M–N–N–R complexes (type **Ia**) is presented in Figs. 2 and 3. The orbital of the M–N–N–R fragment which interacts with an electrophile leading to a type **IIa** complex has amplitude located mainly on the β-nitrogen, whereas less amplitude is found at the α-nitrogen. It should thus be expected that protonation and alkylation of a type **Ia** complex should not affect the bonding patterns significantly. This is in accordance with the structural data for the type **Ia** and **IIa** complexes, in which only small changes in the M–N and N–N bond lengths are observed. The average M–N bond length for 16 **Ia** complexes[6–14] is 1.76 ± 0.02 Å and 1.72 ± 0.02 Å for 7 **IIa** complexes.[6,7,12,17–21]

Finally, with regard to the linear structures, the small deviation from 180° for the M–N–N bond angle should be mentioned. DuBois and Hoffmann have argued that for [MNNR][6] complexes that the MNN angle is coupled to the NNR angle.[32] It was argued that a minimum MNN angle of 172° would give an NNR angle of 120°. An MNN angle of 180° was suggested also to cause an NNR angle of 180°. It was pointed out that the variation in the extent of the π bonding complicates matters in seeking such a correlation.[32]

The interaction diagrams based on the frontier orbitals for the bent structures are shown in Figs. 4, 5 and 6. From the present work, linear M–N–N complexes should be expected to have shorter M–N bond lengths than the bent M–N–N complexes, and this has been borne out experi-

Table 1. Atomic parameters used in the extended Hückel calculations.

	Orbital	H_{ii}	Exponents	
			ζ_{1a}	ζ_{2a}
H	1s	−13.6	1.30	
C	2s	−21.4	1.625	
	2p	−11.4	1.625	
N	2s	−26.0	1.95	
	2p	−13.4	1.95	
O	2s	−32.3	2.275	
	2p	−14.8	2.275	
P	3s	−18.6	1.60	
	3p	−14.0	1.60	
S	3s	−20.0	1.817	
	3p	−13.3	1.817	
Cl	3s	−30.0	2.033	
	3p	−15.0	2.033	
Mo	5s	−8.34	1.956	
	5p	−5.24	1.900	
	4d	−10.50	4.542 (0.58986)	1.901 (0.58986)
Rh	5s	−8.09	2.135	
	5p	−4.57	2.099	
	4d	−12.50	4.290 (0.58070)	1.970 (0.56850)
Re	6s	−9.36	2.398	
	6p	−5.96	2.372	
	5d	−12.66	5.343 (0.63775)	2.277 (0.56576)
Pt	6s	−9.08	2.544	
	6p	−5.48	2.535	
	5d	−12.59	6.013 (0.63307)	2.696 (0.55161)

[a]Exponents in the double zeta-expansion, numbers in parantheses are the coefficients.

mentally.[6-26] Inspection of the structural data for the M−N and N−N bond lengths as well as the M−N−N bond angles for the bent M−N−N complexes reveal that much greater variation is found.[9-12,16,17,22-26] This could be the reason for the different types of complex depicted in Fig. 1. Complexes **IIb**, **IIc**, **IIIa** and **IIIb** are, in principle, the protonated, alkylated, acylated or phenylated form of **Ib** (see **4**, **5**, **6** and **7**). The variation in bond lengths and angles for the bent M−N−N complexes is not as simple to interpret as that for the linear M−N−N complexes. The reason for the greater structural variation in the M−N bond lengths for the bent complexes may be due to the mixing of orbitals in the region 135–115° as shown in Fig. 7. By this mixing of orbitals, especially between the occupied and unoccupied orbitals, great variations in bond length can be expected and we believe that this mixing, to a certain extent, accounts for the structural M−N variations. A simple explanation for the variation in the N−N bond lengths for the bent M−N−N complexes is not feasible as both electronic effects and substitution effects at the nitrogens must be taken into consideration. However, our results for complexes with two similar nitrogen ligands indicate that the bent one should be expected to have a longer N−N bond length than the linear N−N complexes, which is in accordance with the experimental results.[9]

The third group of complexes is the side-on coordinated hydrazido structures. The variation in structures between the titanium and molybdenum complexes is mainly due to the difference in electron density and in the structural environment around the metal.

Appendix

All calculations were performed by the extended Hückel method.[31] The orbital parameters are summarized in Table 1. For all geometries experimental data were used; substituents at phosphorus were modelled by hydrogen, and at the nitrogens either by hydrogen or by a methyl substituent depending on the complex. Standard bond lengths and angles for the substituents on the nitrogens and phosphines were used.

Acknowledgements. Thanks are expressed to the Danish National Science Research Council for financial support (Grant # 11-8377), to Birgit Schiøtt for fruitful discussions and Arne Lindahl for the draft work.

References

1. Sheldon, R. A. and Kochi, J. K. *Metal-Catalyzed Oxidations of Organic Compounds,* Academic Press, New York 1981.
2. Marteel, A. E. and Aawyer, D. T. *Oxygen Complexes and Oxygen Activation by Transition Metals,* Proceedings of The Fifth Annual IUCCP Symposium, Plenum Press, New York 1988.
3. (a) Holm, R. H. *Chem. Rev. 87* (1987) 1401; (b) Jørgensen, K. A. *Chem. Rev. 89* (1989) 431.
4. (a) Sutton, D. *Chem. Soc. Rev. 4* (1975) 443; (b) Dilworth, J. R. and Richards, R. L. In: Wilkinson, G., Stone, F. G. A. and Abel, E. W., Eds., *Reactions of Dinitrogen Promoted by Transition Metals,* in *Comprehensive Organometallic Chemistry,* Pergamon Press, Oxford, UK 1982, Vol. 8, p. 1073.
5. Chatt, J., Dilworth, J. R. and Richards, R. L. *Chem. Rev. 78* (1978) 589.
6. Nicholson, T. and Zubieta, J. *Polyhedron 7* (1988) 171.
7. (a) Douglas, P. G., Galbraith, A. R. and Shaw, B. L. *Trans. Met. Chem. (Weinheim) 1* (1975/1976) 17; (b) Mason, R., Thomas, K. M., Zubieta, J. A., Douglas, P. G., Galbraith, A. R. and Shaw, B. L. *J. Am. Chem. Soc. 96* (1974) 260.
8. Nicholson, T., de Vries, N., Davison, A. and Jones, A. G. *Inorg. Chem. 28* (1989) 3813.
9. Nicholson, T., Lombardi, P. and Zubieta, J. *Polyhedron 6* (1987) 1577.
10. Dilworth, J. R., Harrison, S. A., Walton, D. R. M. and Schweda, E. *Inorg. Chem. 24* (1985) 2594.
11. Fitzroy, M. D., Frederiksen, J. M., Murray, K. S. and Snow, M. R. *Inorg. Chem. 24* (1985) 3265.

12. Dilworth, J. R., Henderson, R. A., Dahlstrom, P., Nicholson, T. and Zubieta, J. A. *J. Chem. Soc., Dalton Trans.* (1987) 529.
13. Dilworth, J. R. and Zubieta, J. A. *Trans. Met. Chem. (Weinheim) 9* (1984) 39.
14. Nicholson, T. and Zubieta, J. A. *Inorg. Chem. 26* (1987) 2094.
15. (a) Gaughan, A. P., Jr., Haymore, B. L., Ibers, J. A., Myers, W. H., Nappier, T. E., Jr. and Meek, D. W. *J. Am. Chem. Soc. 95* (1973) 6859; (b) Gaughan, A. P., Jr. and Ibers, J. A. *Inorg. Chem. 14* (1975) 352.
16. Krogsrud, S. and Ibers, J. A. *Inorg. Chem. 14* (1975) 2298.
17. Nicholson, T. and Zubieta, J. *J. Chem. Soc., Chem. Commun.* (1985) 367.
18. Chatt, J., Dilworth, J. R., Dahlstrom, P. L. and Zubieta, J. *J. Chem. Soc., Chem. Commun.* (1980) 786.
19. Chatt, J., Fakley, M. E., Hitchcock, P. B., Richards, R. L. and Luong-Thi, N. T. *J. Chem. Soc., Dalton Trans.* (1982) 345.
20. Heath, G. A., Mason, R. and Thomas, K. M. *J. Am. Chem. Soc. 96* (1974) 259.
21. Takahashi, T., Mizobe, Y., Sato, M., Uchida, Y. and Haida, M. *J. Am. Chem. Soc. 102* (1980) 7461.
22. Barrientos-Penna, C. F., Einstein, F. W. B., Jones, T. and Sutton, D. *Inorg. Chem. 21* (1982) 2578.
23. Einstein, F. W. B., Jones, T., Hanlan, A. J. L. and Sutton, D. *Inorg. Chem. 21* (1982) 2585.
24. Ittel, S. A. and Ibers, J. A. *J. Am. Chem. Soc. 96* (1974) 4804.
25. Barrientos-Penna, C. F., Campana, C. F., Einstein, F. W. B., Jones, T., Sutton, D. and Tracey, A. S. *Inorg. Chem. 23* (1984) 363.
26. McCleverty, J. A., Rae, A. E., Wolochowicz, I., Bailey, N. A. and Smith, J. M. A. *J. Chem. Soc., Dalton Trans.* (1983) 71.
27. Latham, I. A., Leigh, G. J., Huttner, G. and Jibril, I. *J. Chem. Soc., Dalton Trans.* (1986) 385.
28. (a) Hemmer, R., Thewalt, U., Hughes, D. L., Leigh, G. J. and Walker, D. G. *J. Organomet. Chem. 323* (1987) C29; (b) Hughes, D. L., Jimenez-Tenorio, M., Leight, G. J. and Walker, D. G. *J. Chem. Soc., Dalton Trans.* (1989) 2389.
29. Cowie, M. and Gauthier, M. D. *Inorg. Chem. 19* (1980) 3142.
30. Walsh, P. J., Hollander, F. J. and Bergman, R. G. *J. Am. Chem. Soc. 112* (1990) 894.
31. Hoffmann, R. *J. Chem. Phys. 39* (1963) 1397; Hoffmann, R. and Limscomp, W. N. *J. Chem. Phys. 36* (1962) 2179; *37* (1962) 2872.
32. DuBois, D. L. and Hoffmann, R. *New J. Chem. 1* (1977) 479.
33. Yamabe, T., Hori, K. and Fukui, K. *Inorg. Chem. 21* (1982) 2046.
34. Dilworth, J. R., Garcia-Rodrigues, A., Leigh, G. J. and Murrell, J. N. *J. Chem. Soc., Dalton Trans.* (1983) 455.
35. Mimoun, H., Chaumette, P., Mignard, M. and Sausinne, L. *New J. Chem. 7* (1983) 467.
36. (a) Jørgensen, K. A. and Hoffmann, R. *Acta Chem. Scand., Ser. B 40* (1986) 441; (b) Jørgensen, K. A., Wheeler, R. A. and Hoffmann, R. *J. Am. Chem. Soc. 109* (1987) 3240.

Received May 28, 1990.